

## THE STAR CLUSTERS OF THE SMALL MAGELLANIC CLOUD: STRUCTURAL PARAMETERS

ANDREW HILL\* & DENNIS ZARITSKY

Steward Observatory, University of Arizona, 933 North Cherry Avenue, Tucson, AZ 85721, USA

*To be Published in The Astronomical Journal*

### ABSTRACT

We present structural parameters for 204 stellar clusters in the Small Magellanic Cloud derived from fitting King and Elson, Fall, & Freeman model profiles to the V-band surface brightness profiles as measured from the Magellanic Clouds Photometric Survey images. Both King and EFF profiles are satisfactory fits to the majority of the profiles although King profiles are generally slightly superior to the softened power-law profiles of Elson, Fall, and Freeman and provide statistically acceptable fits to  $\sim 90\%$  of the sample. We find no correlation between the preferred model and cluster age. The only systematic deviation in the surface brightness profiles that we identify is a lack of a central concentration in a subsample of clusters, which we designate as “ring” clusters. In agreement with previous studies, we find that the clusters in the SMC are significantly more elliptical than those in the Milky Way. However, given the mean age difference and the rapid destruction of these systems, the comparison between SMC and MW should not directly be interpreted as either a difference in the initial cluster properties or their subsequent evolution. We find that cluster ellipticity correlates with cluster mass more strongly than with cluster age. We identify several other correlations (central surface brightness vs. local background density, core radius vs. tidal force, size vs. distance) that can be used to constrain models of cluster evolution in the SMC.

*Subject headings:* globular clusters: general — galaxies: star clusters — galaxies: Small Magellanic Cloud

### 1. INTRODUCTION

The study of the structure and evolution of stellar clusters has been reinvigorated by the discovery of young star clusters in ongoing galaxy mergers (Holtzman et al. 1992; Whitmore et al. 1993) and poststarburst systems (Yang et al. 2004). The desire to understand the formation and evolution of these objects, and to use these objects to provide a measure of the time and efficiency of star formation during mergers, provides yet another connection between studies of distant and Local Group galaxies. The Magellanic Clouds contain numerous young clusters that can be studied in detail because of their proximity and can guide our understanding of cluster evolution. A first step in the study of the cluster population is the measurement of such physical characteristics as the surface brightness profiles. We present surface brightness profiles and model fits for 204 clusters in the Small Magellanic Cloud.

Our understanding of the surface brightness profiles of star clusters is dominated by two particular models. The first generically successful set of models was empirically derived to reproduce the surface brightness profiles of Galactic globular clusters (King 1962). These have become known as King profiles and were later derived from tidally limited models of isothermal spheres (King 1966). Consequently they are expected to accurately describe bound stellar systems, if they have isothermal and isotropic stellar distribution functions, stars of the same mass, and reside within a tidal field exerted by another object. Extensions to non-isotropic systems (Michie 1963), rotat-

ing systems (Prendergast & Tomer 1970; Wilson 1975), anisotropic and rotating systems (Lupton & Gunn 1987), and multimass models (Da Costa and Freeman 1976; Gunn and Griffin 1979) exist. Only clusters in the nearest galaxies, including the Milky Way of course, are sufficiently well-resolved to test whether King models, and the corresponding extensions, are proper descriptions. In general, the basic King model is sufficient to explain the observed profiles of Galactic globular clusters, typically a surface density or surface brightness profile, although the extensions have been tested in a few clusters with more detailed observations (for example, using radial velocities in M 13 (Lupton et al. 1987)). As such, they can be viewed either as highly successful fitting formulae to the surface brightness profiles or as self-consistent dynamical models. It is incorrect, however, to infer the full dynamical properties of the King model solely on the basis of a successful fit to the surface density profile.

The second generically successful set of models was empirically derived to reproduce the surface brightness profiles of young ( $< 300$  Myr) clusters in the Magellanic Clouds (Elson et al. 1987; Elson 1991), hereafter EFF profiles. These models have also been successfully applied to young clusters in external galaxies (Whitmore et al. 1999). The lack of the developed tidal cutoff is associated with the cluster’s dynamical youth, although profiles of some old Galactic clusters show similar features at low surface brightness levels that are referred to as extra-tidal stars (Grillmair et al. 1995). When, or even if, a cluster might evolve from an EFF profile to a King profile is unknown and may depend on its environment as well as its individual characteristics. The lack of a well established tidal limit was confirmed for one young LMC cluster (NGC 1866) on the basis of

\*Currently at the Department of Astronomy & Astrophysics, University of Chicago, 5640 S. Ellis Ave, Chicago, IL, 60637  
Electronic address: arhill@uchicago.edu, dzaritsky@as.arizona.edu

stellar kinematics and more marginally suggested for two others (NGC 2164 and NGC 2214; Lupton et al. (1989))

Whether one type of profile is more appropriate for all clusters in the Magellanic Clouds, or whether the appropriate profile depends on cluster age is also unknown because the existing samples of high-quality profiles preferentially include young clusters and because they are small (18 clusters in the LMC (Elson 1991) out of an estimated population of several thousand (Bica et al. 1999), and none in the SMC)<sup>1</sup>. Previous cluster catalogs have identified thousands of clusters in the Large and Small Magellanic Clouds (LMC and SMC; Bica et al. (1999); Pietrzyński et al. (1998); Bica and Dutra (2000)) over a large range of ages (van den Bergh 1981). The combination of structural parameters and ages is critical in unraveling the evolution of these clusters, and by extension the processes that drive cluster evolution in general. Many issues, such as the relationship between core radius and age (Elson et al. 1989) or ellipticity and age (Frenk and Fall 1982) are independent of whether an EFF or King profile is most appropriate at large radius.

Even at the distance of the Magellanic Clouds it can often be difficult to resolve individual cluster stars, and hence both the quality of the data and the details of the model fitting become important. Studies of cluster structure fall into two camps. Either they have used high quality data for a few clusters, such as the study by Mackey & Gilmore (2003a,b) who use *Hubble Space Telescope* images for 10 clusters in the SMC, or they have used photographic plates, such as the study by Kontizas et al. (1982), which achieve a wider field of view but are unable to resolve the inner structure of any cluster. We pursue a study in the middle ground by adopting modern data and algorithms to measure and fit the cluster luminosity profiles, but use ground based data for which determining the structure inside of a few arcsec is limited. We present the necessary basic structural parameters for 204 SMC clusters.

This study has two principal purposes. First, we aim to determine if clusters, particularly those currently dissolving, are still well described by a King profile, and if the older clusters are well described by an EFF profile. Second, aside from issues related to the outer profiles, we present measurements such as core radius and ellipticity that are potentially related to cluster evolution and independent of the detailed shape of the outer surface brightness profile. In addition to the results discussed here, these measurements provide a database from which future, more detailed studies can select targets and form a basis for comparison with other measurements. For example, cluster ages are presented by Rafelski & Zaritsky (2004) and a subsequent study will attempt to place both sets of data within a consistent evolutionary model. In §2 we describe our cluster catalog, in §3 we present our methodology for fitting King and EFF profiles and compare our results to previous studies, in §4 we develop some inferences from the results, and we summarize in §5.

<sup>1</sup> Mackey & Gilmore (2003a,b) have recently obtained high quality surface brightness profiles of 10 SMC and 53 LMC clusters with the *Hubble Space Telescope*, but they note that their profiles do not extend sufficiently far in radius to distinguish between King and EFF models (Mackey & Gilmore 2003a).

## 2. DATA AND CLUSTER CATALOG

The data come from the Magellanic Clouds Photometric Survey (MCPS) described by Zaritsky et al. (1997) and Zaritsky et al. (2002). In summary, we have obtained U,B,V, and I drift-scan images of the central 4.5° by 4° area of the SMC using the the Las Campanas Swope (1m) telescope and the Great Circle Camera (Zaritsky et al. (1996)). The stellar photometric catalog is provided by Zaritsky et al. (2002) and we utilize it and the original images in this study. The effective exposure time is between 4 and 5 min for the SMC scans and the pixel scale is 0.7 arcsec pixel<sup>-1</sup>. Typical seeing is ~ 1.5 arcsec and scans with seeing worse than ~2.5 arcsec were rejected. The final catalog contains over 5 million stars with at least both *B* and *V* measured magnitudes. The astrometry for individual stars has a standard deviation of 0.3 arcsec (derived both from internal errors and comparisons with a variety of external studies, see Zaritsky et al. (2002)).

Although extensive cluster catalogs already exist for the SMC, we performed our own cluster search to examine the completeness of those catalogs over the entire MCPS survey area. The approach we use is similar to that employed for a portion of the LMC by Zaritsky et al. (1997) and for the central ridge of the SMC by Pietrzyński et al. (1998). Specifically, we construct a stellar density image using the stellar photometric catalog. Within 10 arcsec pixels, we count the number of stars with *V* < 20.5. This particular magnitude limit is chosen to minimize spurious detections and spatial variations due to differing levels of completeness within and across different scans. The resulting stellar density image is then median filtered with a box of size 10 such pixels (100 arcsec), and the filtered image is subtracted from the unfiltered image to remove large-scale stellar density fluctuations. We use SExtractor (Bertin and Arnouts 1996) to identify peaks in the residual image and set the parameters generously so that many spurious peaks are found.

Our need in this particular study is for unambiguous clusters for which structural parameters can be measured. Most of the effort in building a cluster catalog goes into recovering and confirming the most marginal objects. As such, some of the clusters published in previous studies are quite dubious and various authors disagree on the validity of these poor clusters (for example, see the cross-comparison of the OGLE catalog (Pietrzyński et al. 1998) with the previous catalog by Bica and Dutra (2000)). Because our aim is to proceed with further detailed study of clusters, we focus on defining a set of robust clusters. From a cross-comparison of our catalog with published catalogs, and then visually inspecting the images of candidates, we settle on the list of 204 clusters presented in Table 1. Of the rejected clusters from our catalog, many match identifications in other catalogs but are either visually unconvincing, too poor to offer much chance of further investigation, or embedded in strong nebular emission. Therefore, exclusion from our list does not necessarily imply that we reject that candidate cluster as a real cluster. The added criteria that we have imposed will preferentially exclude young clusters within emission regions, those embedded in the denser parts of the SMC, and those with a relatively low cen-

TABLE 1  
CLUSTER DESIGNATION AND POSITION

Cluster	RA	DEC	Alternate Designations
1	$0^h 24^m 18.67^s$	$-73^\circ 59' 35.8''$	...
2	$0^h 24^m 43.16^s$	$-73^\circ 45' 11.7''$	K5, L7, ESO28-18
3	$0^h 25^m 26.60^s$	$-74^\circ 04' 29.7''$	K6, L9, ESO28-20
4	$0^h 27^m 45.17^s$	$-72^\circ 46' 52.5''$	K7, L11, ESO28-22
5	$0^h 28^m 02.14^s$	$-73^\circ 18' 13.6''$	K8, L12
6	$0^h 29^m 55.22^s$	$-73^\circ 41' 57.1''$	HW3
7	$0^h 30^m 00.27^s$	$-73^\circ 22' 40.7''$	K9, L13
8	$0^h 31^m 01.34^s$	$-72^\circ 20' 29.0''$	HW5
9	$0^h 32^m 41.02^s$	$-72^\circ 34' 50.1''$	L14
10	$0^h 32^m 56.26^s$	$-73^\circ 06' 56.6''$	NGC152, K10, L15, ESO28-24

NOTE. — The complete version of this table is in the electronic edition of the Journal. The printed edition contains only a sample.

tral surface brightness. This sample is not complete, nor necessarily representative of the overall population, but the biases are qualitatively understood and the sample is still far larger than any for which detailed structural parameter fits are available.

For the crossidentification presented in Table 1, we identify the closest cluster in projection from the Bica and Dutra (2000) catalog which contains clusters, association, and some other sources such as planetary nebulae. For matches, the coordinates typically differ by a few arcsec, well within the quoted general uncertainty of 10 arcsec (Bica and Dutra (2000)).

### 3. PROFILE FITTING

#### 3.1. Methodology

Although we fit both King and EFF profiles to our clusters, we place greater emphasis on the King profiles for several reasons. First, the full set of King models include profiles with extended wings. The largest concentration models we fit resemble a power law profile with an effective index similar to the typical EFF profile (see Figure 1). Second, previous studies have only demonstrated that the youngest LMC clusters, those with age  $< 300$  Myr, are better fit by an EFF profile, while over half of our cluster sample is estimated to be older (Rafelski & Zaritsky 2004). Finally, focusing on a single family of models allows for a more straightforward comparison across the sample. Our decision to emphasize the King profile is certainly open to critique, particularly if the data were to favor the EFF profile. Our results indicate that this is not the case. If the surface brightness profiles of young clusters are better fit by softened power law profiles, we should find these clusters more successfully fit by increasingly concentrated King models. However, our analysis shows King models are not only statistically satisfactory fits for  $\sim 90\%$  of the clusters, but also are generally superior fits than EFF profiles for the bulk of the sample (see §3.2).

The usual approach of fitting a model profile to the surface density of a cluster is complicated by the incompleteness of our stellar catalog that results from crowding in the centers of many clusters. We overcome this difficulty by fitting models to the surface brightness profile rather than attempting the difficult and inherently

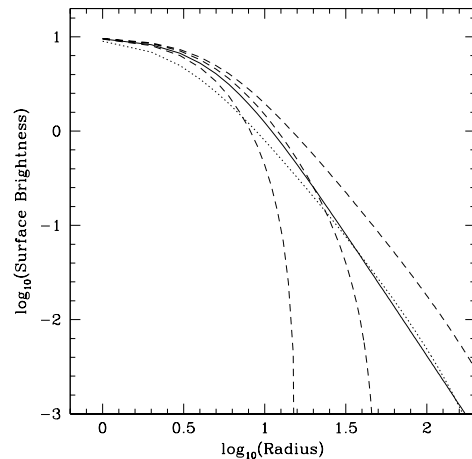


FIG. 1.— A comparison of King and EFF profiles (arbitrary units). The short dashed lines represent King models with  $c = 0.52, 1, 2.1$  and an identical core radius (5), with increasing  $c$  going from left to right. The solid line represents an EFF profile with the same value for  $a$  and a value of  $\gamma$  typical for young clusters, 2.6 (Elson et al. 1987). The dotted line represents a King model with  $c = 2.1$  and a core radius adjusted to result in an outer profile that agrees well with that of the EFF model.

uncertain task of defining and applying an incompleteness correction. We choose to work with the  $V$ -band images because they are the deepest of our set, and because  $V$  is more sensitive to the underlying stellar populations than either  $U$  or  $B$  while being less sensitive to foreground contaminating stars than  $I$ . Furthermore, use of  $V$  allows us to compare directly to previous studies (Kontizas et al. 1982; Kontizas & Kontizas 1983; Kontizas et al. 1986; Mackey & Gilmore 2003b) without concern for possible color gradients.

Obtaining an accurate determination of each cluster's center is the first step in constructing the surface brightness profile. We use the approximate coordinates given in our catalog to extract a  $350'' \times 350''$  image of the cluster. A precise center is determined by calculating the luminosity-weighted centroid. To avoid spurious results due to contamination by other clusters or bright foreground stars, we constrain the calculation to pixels within  $20''$  of the approximate center and exclude pixel values that are 3000 counts above the mode of the entire frame (typical mode values are between 100 and 200 counts). We iterate four times, with each successive run using the previous luminosity-weighted center. The derived centers are stable. For some irregular clusters, we adjust the center to match a visually identified center that corresponds to central condensation of stars, rather than a broader luminosity centroid. This adjustment is typically not more than a few arcsec.

As has been previously noted (Frenk and Fall 1982), many SMC clusters are elliptical. The nature of this ellipticity, whether it is fundamentally connected to age or luminosity, is debated (Elson 1991; van den Bergh and Morbey 1984). Despite the conclusion from Elson (1991) that the asphericity primarily re-

sults from unrelaxed stellar concentrations rather than any true underlying elliptical light distribution, we opt to effectively use elliptical isophotes in determining our surface brightness profile. Because we model the surface brightness of the cluster, subconcentrations should be considered both in determining whether a profile is a good fit and whether elliptical isophotes are necessary.

The ellipticity and position angle of each cluster are determined by computing the second moments of the cluster luminosity distribution (see Banks et al. (1995) for a similar treatment of a small sample of LMC clusters). We restrict the computation to pixels with fewer than 5000 counts above the mode, and to radii between  $3''$  and  $0.7r_t$ , where  $r_t$  is the fitted tidal radius, or  $30''$  on the first iteration of this procedure. These criteria are selected with the intention of minimizing the effect of background and foreground contamination and ignoring the seeing-smoothed inner radii. The ratio of the eigenvalues of the matrix formed from the second moments of the luminosity distribution is the projected ratio of the semi-minor,  $b$ , to semi-major,  $a$ , axis of the cluster, while the eigenvector matrix is the rotation matrix of the cluster. Using these results, we rotate the image so that the major axis lies along the horizontal axis and scale the image along the vertical axis by  $a/b$ .

We compute the surface brightness profiles using circular annuli of  $2''$  width and adopt an uncertainty that is given by  $\sigma$  of the mean of the pixel values within that annulus. We exclude pixels with more than 12000 counts above the mean for the annulus to eliminate contamination from the brightest stars. We choose different pixel thresholds for our calculation of the center, ellipticity, and surface brightness because of different sensitivities to non-cluster objects. Surface brightness profiles are measured out to  $200''$  and include a substantial sky region for all clusters.

The determination of the sky level is key in assessing the nature of the outer regions of the surface brightness profiles of clusters. As shown in Figure 2, an error equivalent to 10% of the central surface brightness of the cluster can convert an intrinsic EFF profile into an apparently tidally truncated profile or an intrinsic King profile into an apparent one with no tidal radius. Errors in the background that are less than 1% of the cluster's central surface brightness do not qualitatively affect the nature of the outer radial profile. It is important to note that this is a statistical uncertainty that also affects, but was ignored by, previous studies. We measure the background using an outer annulus that typically extends over the last quarter of the radial range of the extracted images ( $r > 150''$ ), although we adjust the boundaries of the sky region interactively for large clusters or for those with contaminating stars. Because young stars are spatially correlated (Harris & Zaritsky 1999), going to larger and larger radius to measure the background is not an appropriate solution, particularly for the younger clusters where the spatial correlations are the strongest. Moreover, there is no reason to expect the background at large radii from the cluster to be the same as the background in which the cluster resides, especially if there are many young stars in the region. Unfortunately, adopting background annuli near the clusters can often result in background measurements that are affected by local fluctuations. The determination of the background is therefore

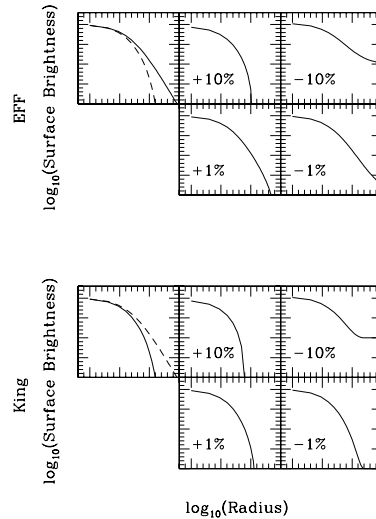


FIG. 2.— A comparison of the effect of background subtraction errors on both representative King and EFF profiles. Upper set of panels illustrate the effect of oversubtracting (+) and undersubtracting (−) the background by a percentage of the central brightness of the cluster on EFF profiles (the original profile is represented by the solid line in the upper left panel). The dashed line represents the comparison King profile in the upper panel and the comparison EFF profile in the lower panel. The lower panels are analogous except for illustrating the effect of background errors on a King profile.

an inherently poorly solved problem. We opt against including the background as a free parameter in the model fitting described below because we find that including radial bins in which the background dominates allowed us to improve the statistical measure of the fit, although it often introduces systematic errors in the fitted cluster profile. This problem arises because the photometric properties of the area around the cluster are not necessarily identical to those underlying the cluster, in particular the background is not uniform. A statistical fitting method attempts to fit the background at the expense of fitting the cluster and results in fits that are visually inferior in many cases. Including only radial bins in which the cluster dominates results in fitting degeneracies due to the lack of a strong direct constraint on the background level. Instead, we determine the background independently from a sky annulus at moderate radius, which is similar to the procedure adopted by EFF. The inner boundary of our sky region is typically about 8 times larger than the radius that includes 90% of the cluster light. Our fits to the background, and the comparison benchmarks of 1 and 10% errors, are shown in Figure 3. The Figure illustrates that there are some clusters for which the scatter in the background exceeds the 10% benchmark and hence sky uncertainties play a significant role, while there are others for which the scatter is less than the 1% benchmark and hence sky uncertainties are sufficiently small that the outer cluster profile is well measured.

We fit King and EFF profiles to each of our clusters via chi-squared minimization. The standard King model is described by a combination of three parameters (King 1966). We choose to define each profile by its central

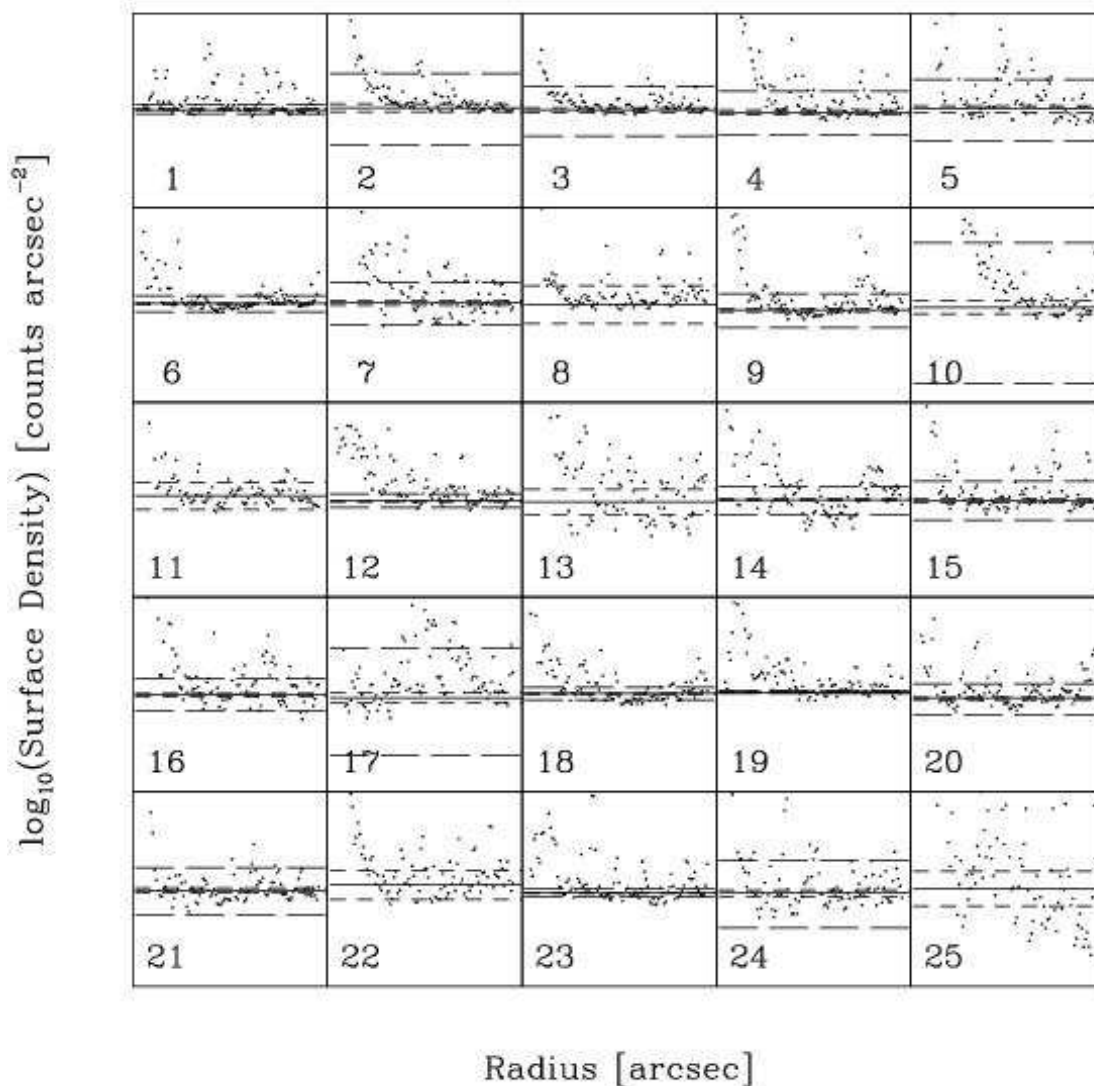


FIG. 3.— Background fits for the first 25 SMC clusters (numbers in lower right are the cluster designation). The range of horizontal axis is from 0 to 200 arcsec for all clusters. The vertical scale is unique for each cluster and corresponds to  $\pm 10\%$  of the selected background value. The sky used in our fitting is shown by the solid line. The short dashed line mark the range of error corresponding to 1% of the central surface brightness of the cluster and the long dashed lines correspond to 10%. We show a representative sample here and present all the clusters in the electronic version of the Figure.

surface brightness,  $\Sigma_0$ , core radius,  $r_c$ , and concentration,  $c$ . Other common parameters, such as tidal radius, can be derived from this set (ie.  $c \equiv \log_{10}(r_t/r_c)$ ). In addition to these three parameters, our profiles include the background surface brightness discussed above. We explore a parameter space that ranges in  $\Sigma_0$  from 0.25 to 1.75 times the mean  $\Sigma$  measured within the central  $4''$  of the cluster in increments of 0.025, in  $r_c$  from  $1''$  to  $101''$  in increments of  $0.5''$ , and in  $c$  from 0.001 to 2.1 in increments of 0.01. The concentration range corresponds to the range over which King's original empirical models match his theoretical models as found by Wiyanto et al. (1985). The fitting is iterated once. Error bounds on each best fit parameter corresponds to the range of that parameter among models that cannot be rejected with

more than 67% confidence.

As mentioned above, Elson et al. (1987) noted that the surface brightness profile,  $\mu(r)$ , of young clusters appear to be better described by a core plus power law profile,  $\mu(r) \propto (1 + r^2/a^2)^{-\gamma/2}$ , where  $a$  and  $\gamma$  are free parameters. We fit the EFF models our data in the same manner as we fit the King profiles, over the same radial range, by varying the central density ( $\Sigma_0$ ), the scale length ( $a$ ), and the power-law index ( $\gamma$ ). Note that  $a$  is the scale length, rather than the core radius, which can be calculated using  $r_c = a\sqrt{2^{2/\gamma} - 1}$ . We explore a parameter space that ranges in  $\Sigma_0$  from 0.25 to 1.75 times the mean  $\Sigma$  measured within the central  $4''$  of the cluster in increments of 0.025, in  $a$  in from  $1''$  to  $101''$  in increments of  $0.5''$ , and in  $\gamma$  from 1.5 to 7.0 in increments of 0.05.

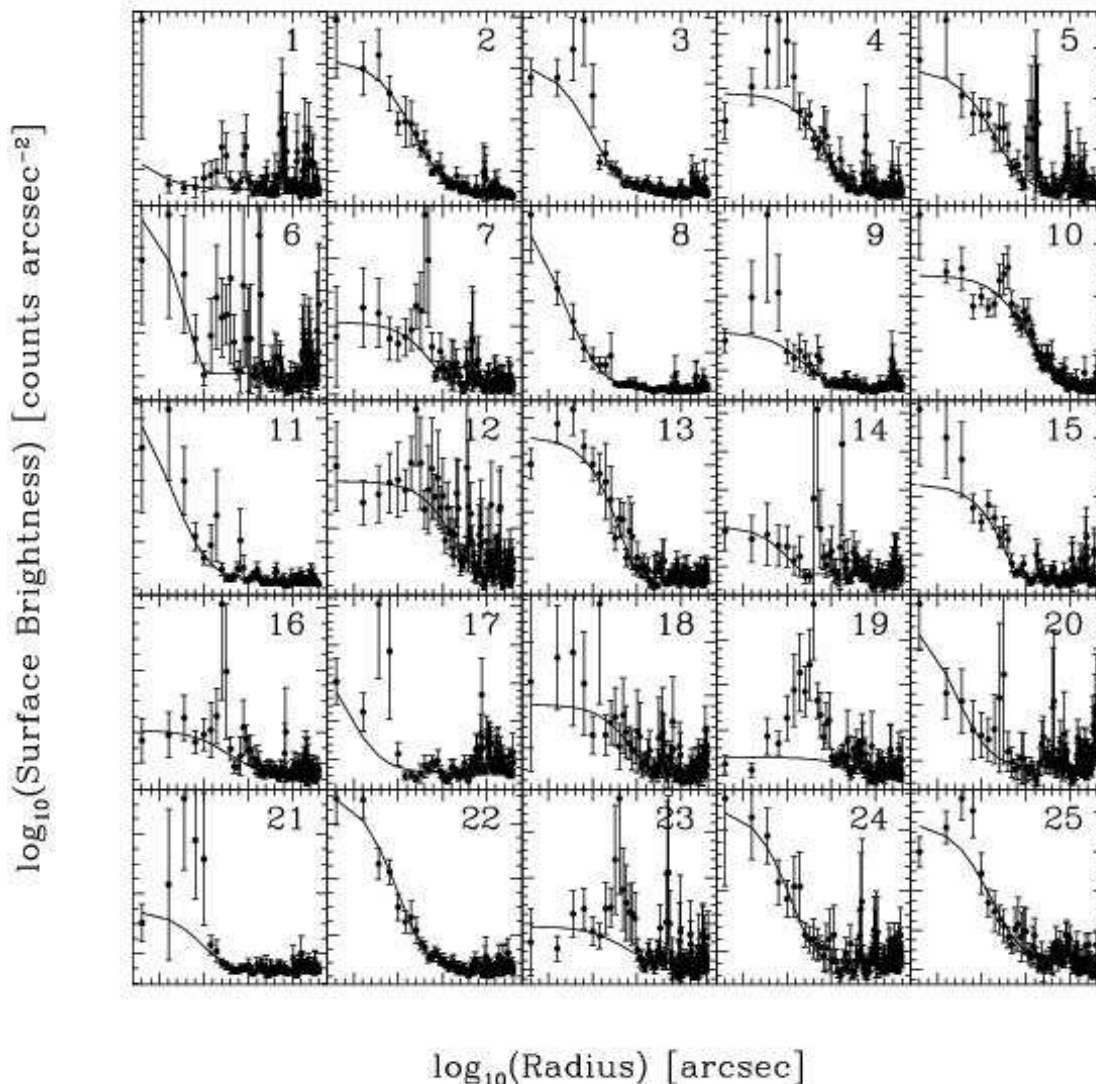


FIG. 4.— V-band surface brightness profiles of the first 25 SMC clusters and profile fits. These profiles include the background flux. The range of horizontal axis is from 0 to 200 arcsec for all clusters. The vertical scale is unique for each cluster. The central surface brightness of each cluster fit is given in Table 2. The best fit King profile is shown by the solid line. The numeral in the upper right of each panel provides the cluster identification. We show a representative sample here and present all the clusters in the electronic version of the Figure.

We present the best fit King profiles in Figure 4 and both King and EFF profiles in Figure 5 overlaid on the data. The key difference between the two Figures is that Figure 4 shows the un-background subtracted data so that all of the data could be plotted on the logarithmic scale. Note however, the profiles plotted in this manner do not resemble the standard King models, although they are. In Figure 5 we again plot the background-subtracted profiles, but here we stop plotting data and models once a radial bin has a negative background subtracted value because the logarithm is undefined. Plotting only data greater than the background, i.e. those with positive background subtracted values, results in a misleading profile. The parameter values for the fits are presented in Table 2. The  $1\sigma$  confidence intervals are defined using  $\chi^2$ , and are therefore undefined in the cases

where even the best fit model has  $\chi^2$  greater than the corresponding value for the available degrees of freedom.

### 3.2. Results

Of the 204 clusters in our catalog, only 44 are poorly described by a King profile with greater than 67% confidence. Given the size of our sample however, we expect from statistical considerations that a substantial number of clusters that are truly well described by a King profile will be rejected at this level. We calculate that only 19 clusters are fit sufficiently poorly that for each individual cluster the King profile can be rejected as an accurate description of their surface brightness profile (this limit corresponds to rejecting the profile with 99.5% confidence). Because both the King and EFF profiles can fit clusters with extended radial surface brightness profiles,

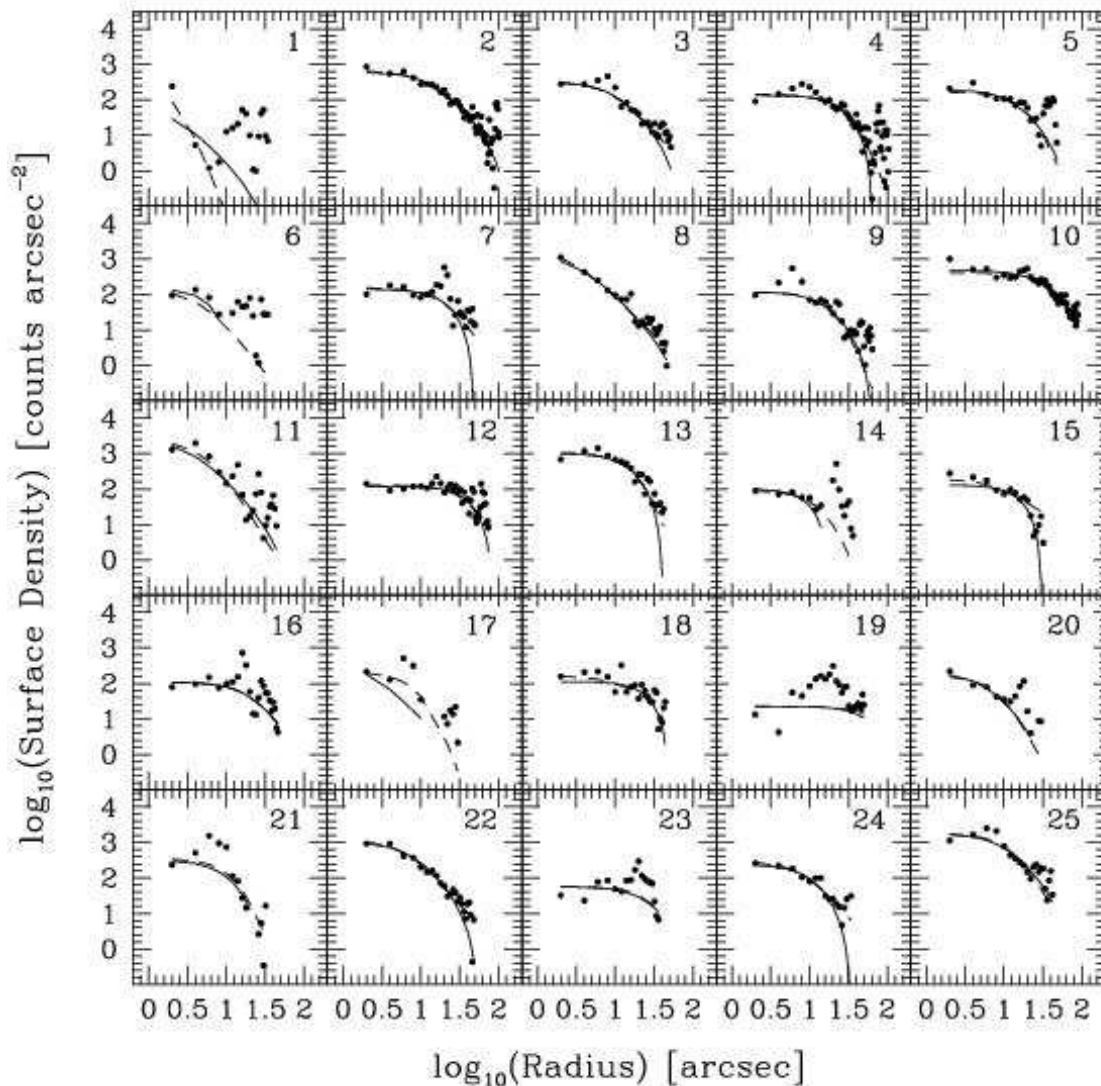


FIG. 5.— The V-band cluster profiles, after background subtraction, are compared to both the best fitting King (solid line) and EFF profiles (dashed line). The radial plots are truncated at the innermost radius for which the counts minus the background are less than zero to avoid only plotting values for which the logarithm exists. This omission results in some profiles that appear to be systematically poor fits because the fit includes data that are omitted from the Figure. Error bars have been omitted for clarity. All panels are identically scaled and the numeral in the upper right corner provides the cluster identification. All cluster profiles are available in the electronic version of this Figure.

the profile itself cannot be used to infer extratidal stars (i.e. stars beyond the cluster’s Roche lobe). While the extended wings in the EFF profile are generally interpreted to arise from that type of mass loss, the extended wings in a high-concentration King model are bound to the system. Determining which physical interpretation is correct will require either direct dynamical measurements, such as a measurement of the cluster mass and the velocity dispersion of stars, or indirect evidence, such as a lack of old clusters with such wings, which would imply that there has been dynamical evolution of such clusters. In this study, we reach conclusions on the relative merits of the fitting functions, not on the dynamical state of the clusters. As we have illustrated before (Figure 1), describing a surface brightness with a King profile does

not necessarily imply the presence of a dramatic tidal edge.

We find that our determination of the tidal radius is highly uncertain. This uncertainty arises from the strong coupling of the estimated  $r_t$  to the determination of the background. Similarly, the uncertainty on the concentration, because it depends on  $r_t$ , is too large to be meaningful. Because we desire a robust measure of cluster size, we pursue an alternative definition of size determined by the enclosure of a significant fraction of the total cluster light, rather than all of the light. We choose to tabulate the radius inside of which 90% of the total cluster luminosity of the *fitted profile* is contained,  $r_{90}$ . Even though  $r_{90}$ , by definition, still contains the bulk of the cluster light, the associated uncertainty is typically half that of  $r_t$ . We

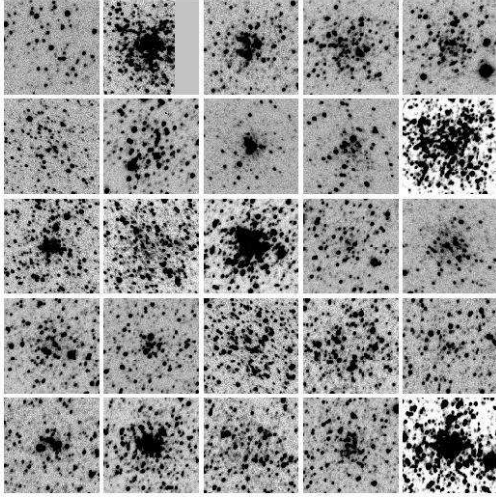


FIG. 6.—  $V$ -band images of the first 25 SMC clusters. The angular size of each image corresponds to the central quarter of the area for which the profiles in Figure 4 are derived. Images of all the clusters in the four filters are available in Rafelski & Zaritsky (2004).

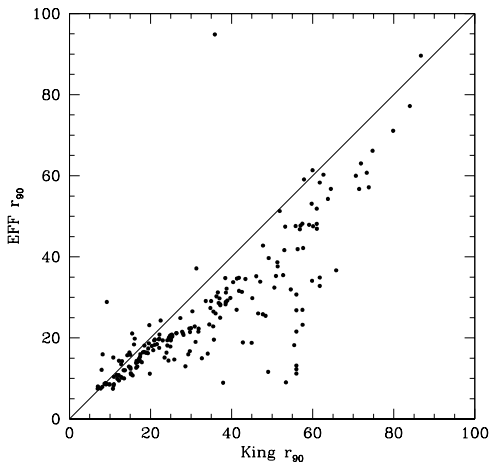


FIG. 7.— Comparison of  $r_{90}$  values obtained with the King and EFF models. The solid line is the 1:1 line.

avoid going to even smaller radii because then connection to the cluster size becomes increasingly tenuous and dependent on the cluster profile. Because of the ambiguity of which model profile to use, one may wonder whether defining  $r_{90}$  using one profile or the other leads to large differences in the calculated value of  $r_{90}$ . We show in Figure 7 a comparison of the values of  $r_{90}$  obtained using the best fit King or EFF model. We find that although there is some systematic difference between the two that can be as large as 25%, the rankings of clusters according to size (and hence any correlation one might examine using

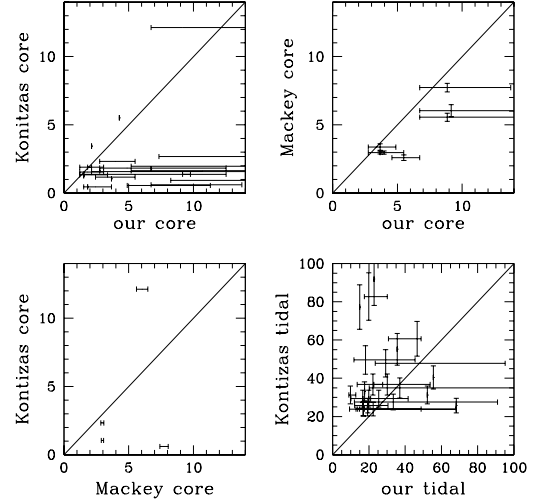


FIG. 8.— Comparison of our measured core and tidal radii to previously published values. Our core radii are compared to those presented in Kontizas et al (1982,1983,1986) in the upper left panel and those measured by Mackey & Gilmore (2003b) in the upper right. The core radii of Kontizas et al and Mackey & Gilmore are compared at bottom left. The bottom right panel features a comparison on our tidal radii to those published by Kontizas et al. Clusters at (135,26) in the upper left and (55,207) in the bottom right were excluded for clarity.

$r_{90}$ ) is maintained to large degree regardless of the model one adopts. The best fit parameters for each candidate, along with the  $1\sigma$  uncertainties, are presented in Table 2. The listed magnitude is calculated by integrating the fitted King profile. The complete set of profiles, images, and structural parameters is presented in the online version of these Figures and Tables.

Our measurements of structural parameters constitute the largest such survey of SMC cluster profiles, so the availability of comparison data is limited. There exist only four published studies of SMC cluster profiles, three of which are by a single group of authors and should be considered a single survey. Kontizas et al. (1982), Kontizas & Kontizas (1983), and Kontizas et al. (1986), hereafter collectively referred to as Kontizas et al., use photographic plates from the U.K. Schmidt and Anglo-Australian telescopes in Australia to measure 67 cluster profiles, while Mackey & Gilmore (2003b) present 10 profiles measured from images obtained with the *Hubble Space Telescope*. All 10 clusters observed by Mackey & Gilmore (2003b) appear in Kontizas et al., but most were observed using different filter passbands. Although we do not know whether the structural parameters are strongly dependent on color, a conservative comparison should be limited to parameters determined from images taken with similar filters. An examination of Kontizas et al.'s observations in a variety of filters and emulsions do suggest that a cluster's profile may depend on the wavelength in which it is observed, although this issue is not specifically investigated. We restrict our comparison to the smaller set of 28 clusters observed in a filter and emulsion combination closely corresponding to our  $V$ -band observations. Our cluster sample includes



TABLE 2  
STRUCTURAL PARAMETERS<sup>a</sup>

Cluster	Core Radius [pc]			90% Light Radius [pc]			$M_V$	$\Sigma_{0,K}$ [cts/ arcsec <sup>2</sup> ]	$\epsilon$	$\chi^2_{\nu,K}$	EFF Scalelength <sup>b</sup> [pc]			$\gamma$			$\Sigma_{0,E}$ [cts/ arcsec <sup>2</sup> ]	$\chi^2_{\nu,E}$
	low	best	high	low	best	high					low	best	high	low	best	high		
1	0.61	0.61	0.92	11.58	15.56	17.34	18.7	60	0.30	0.99	...	0.76	...	...	6.30	...	421	1.24
2	2.44	3.97	7.33	12.17	18.06	20.84	12.9	595	0.17	0.77	1.07	3.35	8.37	1.50	2.20	4.65	659	0.70
3	...	2.75	...	...	...	11.30	...	314	0.02	1.25	...	2.59	...	...	2.45	...	335	1.93
4	5.19	10.69	18.94	11.54	12.62	16.69	13.8	133	0.18	0.81	...	13.01	...	...	6.95	...	144	1.50
5	1.53	3.97	12.52	6.43	11.90	19.20	14.8	189	0.28	0.68	1.22	8.52	10.96	1.50	6.90	7.00	167	0.73
6	0.61	3.36	14.97	10.39	18.31	24.30	16.9	145	0.37	0.79	0.61	1.37	12.94	1.50	2.75	7.00	135	0.82
7	9.16	9.16	9.77	9.57	9.57	9.62	14.5	139	0.56	1.10	3.51	6.55	11.87	1.85	3.40	7.00	153	1.08
8	0.92	0.92	1.53	7.08	11.78	14.98	14.7	1259	0.38	0.87	0.61	0.76	1.83	1.80	2.20	3.10	1835	0.87
9	2.75	4.89	12.52	6.99	11.24	12.81	14.8	116	0.37	0.70	3.20	8.68	10.50	2.25	7.00	7.00	116	0.87
10	6.72	9.16	14.36	19.82	22.40	24.11	12.1	474	0.23	0.79	...	18.57	...	...	6.30	...	399	1.35

NOTE. — The complete version of this Table is in the electronic edition of the Journal. The printed edition contains only a sample.

<sup>a</sup>The  $1\sigma$  confidence intervals are defined using  $\chi^2$ , and are therefore undefined in the cases where even the best fit model has  $\chi^2$  greater than the corresponding value for the available degrees of freedom.

<sup>b</sup>The core radius, when defined as the radius for which the surface brightness drops to half its central value, can be calculated using  $r_c = a\sqrt{2^{2/\gamma} - 1}$ .

25 from this restricted set.

Our measurements of  $r_c$  and  $r_t$  are compared to those made by Kontizas et al. and Mackey & Gilmore (2003b) in Figure 8. Our core radii are systematically larger than those measured by Kontizas et al. This result is consistent with Kontizas et al.’s prediction that their core radii are underestimated, a conclusion also reached by Mackey & Gilmore (2003b). Given that Kontizas et al. could not resolve the core in any of their clusters, it is not surprising that there is disagreement with both our measurements and those of Mackey & Gilmore (2003b). More illuminating is the comparison of  $r_c$  measurements with those of Mackey & Gilmore (2003b), who are able to resolve the inner regions of the clusters. Here we find that our results are statistically consistent, although with some slight bias to overestimate  $r_c$  by  $\sim 30\%$ . We suspect that our core radii are systematically larger because we are unable to resolve the inner cluster structure to the degree possible in the *HST* observations.

Comparison of tidal radii is more uncertain both because there is a smaller set of data with which to compare to and the lack of modern techniques used in constructing smaller comparison set. Although the Mackey & Gilmore (2003b) observations do not extend to large enough radii, Kontizas et al.’s do. Figure 8 reveals that our tidal measurements are consistent with, although  $\sim 20\%$  systematically smaller than, those reported by Kontizas et al. Given the lack of precision with which tidal radius can be fit (see §3.2), this difference is not surprising, especially given the significant difference in the quality of the data and analysis techniques between our study and that by Kontizas et al. We conclude that our model fits are in rough accord with previous fits, but given the size of the scatter seen in Figure 8 and our calculated uncertainties for  $r_t$  we do not include  $r_t$  values in Table 2.

We now return to the issue of the appropriateness of the King model. There are two fundamental issues: 1) does the King profile provide an acceptable description of the surface brightness profile and 2) does the King model provide an acceptable description of the stellar

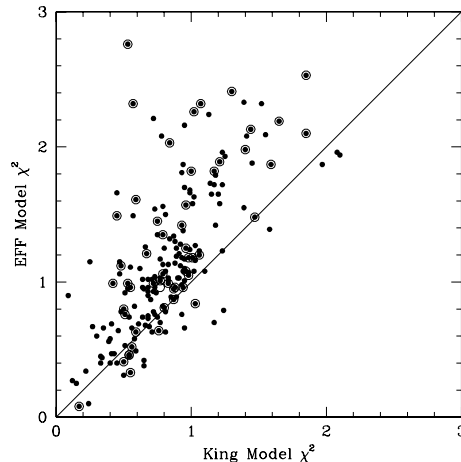


FIG. 9.— The  $\chi^2_{\nu}$  values for the best fit King and EFF profiles. The line is the 1:1 line. Only clusters for which the fits have  $\chi^2_{\nu} < 3$  are shown. Those clusters with background values determined to be better than 1% of the central cluster surface brightness are plotted with larger open circles surrounding the central filled circle.

dynamics. With our data, we are only in a position to address the former of these. Indeed, dynamical considerations would suggest, as noted above, that King models are unlikely to be the correct dynamical description of the younger clusters. For the bulk of the clusters there are only subtle differences between the King and EFF profile that mostly occur near the outer edge of the clusters, in the region where the background uncertainties may dominate. The fit in this region is not shown in Figure 5 because we stop plotting once the background subtracted flux value is less than zero, and is hence undefined in the units plotted. However a comparison of the  $\chi^2_{\nu}$  values, Figure 9, demonstrates that while for any individual cluster the  $\Delta\chi^2_{\nu}$  is typically not large enough to

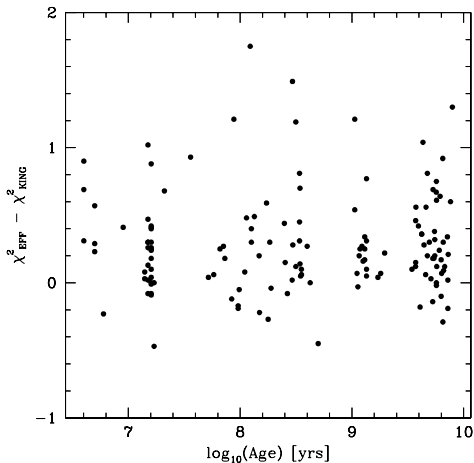


FIG. 10.— The  $\Delta\chi^2_{\nu}$  values vs. age. We include only clusters for which either the King or EFF models fit with  $\chi^2_{\nu} < 1$  and  $\Delta\chi^2_{\nu} < 2$ .

rule out one model relative to the other, the King model systematically fits these cluster profiles better. To address the importance of the background subtraction to this conclusion, we have highlighted in the Figure the clusters for which the background is determined to better than 1% of the cluster’s central surface brightness (an uncertainty level below which the cluster profiles do not appear to be grossly disturbed by incorrect background subtraction, see Figure 2). These high quality surface brightness profiles follow the mean trend. In the cases where the King model does significantly better than the EFF models and the cluster is a rich cluster with a well determined sky brightness and overall profile, the difference in the models is clearly in the outermost regions (see for examples clusters 85, 86, 96, 143, 174). In other cases, the cause for the preference of the King model is more subtle and ambiguous. It is presumably due to a cumulative effect in the fit over the range between core and tidal radius.

To examine whether one particular model is favored for clusters of a particular age, for example EFF models for the youngest clusters, we have plotted the difference in  $\chi^2_{\nu}$  values as a function of age (ages from Rafelski & Zaritsky (2004)) in Figure 10 for fits where either the King or EFF model had  $\chi^2_{\nu} < 1$ . There is no trend evident that favors one particular model at a specific age. The general preference for King models ( $\Delta\chi^2_{\nu} > 0$ ) is seen at all ages. Of course this result doesn’t argue against the effectiveness of the EFF profile for some clusters, nor against the existence of some clusters that are not tidally limited. Nevertheless, the situation is clearly more complicated than an expectation that all young clusters should have power-law surface brightness profiles.

#### 4. DISCUSSION

##### 4.1. Cluster Subpopulations

Even those clusters that are well-fit by a King profile are not drawn from a single parameter population. Al-

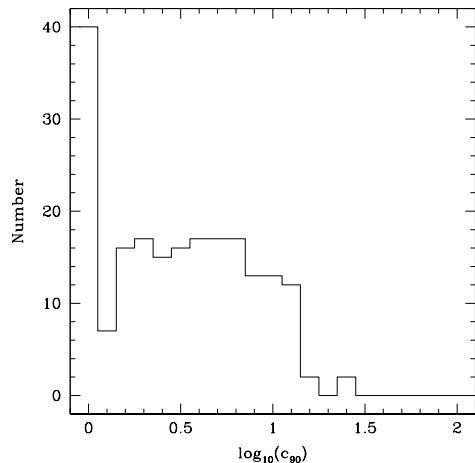


FIG. 11.— The distribution of cluster concentrations in the SMC. Note that  $r_{90}$  as opposed to tidal radius is used to calculate the concentrations for this Figure, while the standard definition of concentration is fit in the model. The axes are set so that the entire range of allowable values of concentration is shown.

though the core radius,  $r_c$ , and  $r_{90}$  are correlated at the 92.7% confidence level (Spearman rank test; see Table 3), clusters distribute themselves over the entire range of  $r_{90}/r_c$  that we allow in our fitting space given the theoretical constraints described by Wiyanto et al. (1985) (Figure 11). This implies that a variety of factors influence the observed structural parameters. Possible influences include tidal effects, age (the internal dynamical evolution of the cluster), and initial conditions (substructure, velocity anisotropies, initial stellar mass function, angular momentum, and chemical abundance). These are notoriously difficult to disentangle, but the large, uniform sample presented here offers a new opportunity to search for clues.

We find King profiles to be a statistically acceptable fit to clusters that range over a factor of over 40 in  $r_c$ , 10 in  $r_{90}$ , and  $10^3$  in  $\Sigma_0$ . This finding is somewhat surprising in light of the fact that the vast majority of clusters are inferred to be in the process of dissolution or disruption on the basis of the cluster age distribution (Boutloukos & Lamers 2003; Rafelski & Zaritsky 2004) and many have had insufficient time to dynamically relax. Therefore, the fits to some clusters are almost certainly not physically meaningful, but rather are statistically allowed given the large observational uncertainties. Nevertheless, even in these cases our measurements do reflect the size of the cluster and its core. Although the large majority of SMC clusters are adequately fit by simple King profiles, and hence demonstrate that measuring surface brightness profiles alone is not a promising avenue to identifying dissolving clusters, there are several populations of clusters that merit further discussion and may be showing signs of their dynamical evolution.

##### 4.1.1. The Ring Clusters

A subset of our cluster luminosity profiles contain a significant bump in the luminosity profile relative to the

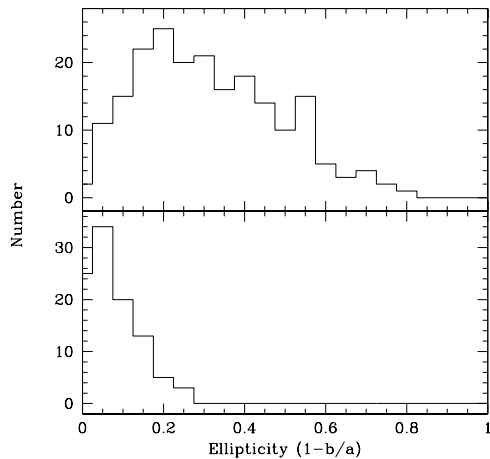


FIG. 12.— The distribution of cluster ellipticities in the SMC and MW. The SMC distribution is depicted in top panel while that of the MW appears in the bottom panel. The MW data come from ?

fitted King or EFF profile. Of those, visual inspection suggests that about 12 out of the 204 have a bump that occurs beyond the central 8 arcsec and is not apparently due to a few luminous stars (clusters 12, 19, 39, 102, 115, 148, 164, 179, 183, 186, 196, and 203 in Figure 4). Although the apparent ring features in some of these clusters may be due to statistical fluctuations, there are at least some where the central deficit of stars is quite evident (see clusters 19, 39, 148, and 186 in Figure 17) and the  $\chi^2_\nu$  values, for these clusters, are larger than expected for random fluctuations in a sample of this size with 99.5% confidence for either the King or EFF profiles (see §3.2). We discount similar features at small radius, for example in clusters 3 and 4, because they could arise from slight centering offsets or random fluctuations within the small inner annuli. We also have not included some clusters in which the profile bump appears to be due to bright contaminating stars (such as cluster 82). Nevertheless, there may be many more clusters in the sample than the 12 listed in which the bump is a real feature. One of the best examples of this phenomenon is cluster 19 (Figures 4, 6, and 17). This feature may be a signal of a cluster’s dissolution because such a configuration appears to be difficult to maintain in equilibrium. Further dynamical modeling is required to confirm this supposition. Aside from dynamical issues, it is also the case that because we fit to the luminosity profile rather than the stellar density profile, we are susceptible to variations in the mass (or number) to light ratio. The degree to which the underlying light profile departs from a King or EFF profile may not indicate a similarly strong deviation in the mass profile.

#### 4.1.2. The Elliptical Clusters

The distribution of cluster ellipticities is presented in Figure 12. To explore the origin of the apparent broad distribution relative to that of the Galactic clusters (data from the compilation of Harris (1996)), we search for sig-

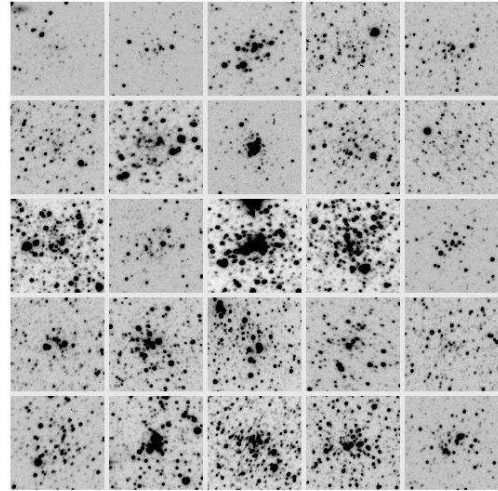


FIG. 13.— V-band images of the 25 most elliptical clusters in the sample

nificant correlations between ellipticity and other cluster properties. For example, ellipticity has been found to correlate inversely with age (Frenk and Fall 1982), which suggested either evolutionary changes in the structure of clusters or changes in the conditions of formation. In a different interpretation of the same correlation, Elson (1991) suggested that subclumps at various stages of merging may produce the impression of large ellipticity in LMC clusters. This conclusion was based on the inverse correlation between age and ellipticity and the interpretation of various features in cluster profiles. However, van den Bergh and Morbey (1984) find that although ellipticity and age are indeed inversely correlated, that result is a byproduct of the inverse correlation between ellipticity and luminosity, a claim not addressed by Elson (1991). However, it is quite difficult to work in terms of luminosity since it depends both on mass and age, both of which might help determine the ellipticity.

In Figures 13 and 14 we present the images of the 25 most and least elliptical clusters. The most elliptical clusters are in general also highly irregular, as well as of low luminosity. The least elliptical clusters are in general, although not exclusively, richer systems. While there are comparably poor, low luminosity systems that are both of high and low ellipticity, the luminous systems appear to uniformly avoid the upper tail of the ellipticity distribution. Two examples of rich clusters with moderately high ellipticities ( $\sim 0.2$ ) are presented in Figure 15. These are among the most elliptical of the rich clusters in the SMC and interestingly correspond to the highest ellipticities measured for Galactic clusters.

We use the age dating results of Rafelski & Zaritsky (2004) to examine whether age or mass is the primary driver of ellipticity. We have converted the age and luminosity measurements from Rafelski & Zaritsky (2004) for the  $Z = 0.004$  models into a mass by using the same Starburst99 models (Leitherer et al. 1999) used to esti-

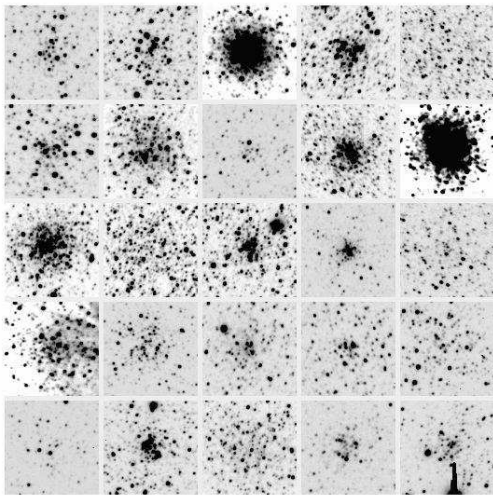


FIG. 14.— V-band images of the 25 least elliptical clusters in the sample

mate the ages. In Figure 16, we plot ellipticity vs. mass for different age bins. The three bins are defined such that the youngest bin contains clusters whose 90% upper confidence age is less than 500 Myr, the middle bin contains clusters whose best fit age is between 1 and 3 Gyr, and the oldest bin contains clusters whose 90% lower confidence age is greater than 3 Gyr. The mean ellipticity of clusters in the three age bins are 0.31, 0.27, and 0.32 (from youngest to oldest), and so we find no correlation between age and ellipticity. On the other hand, all three age bins show some sign of a correlation with mass. All the data together results in a significant detection of an inverse correlation (Spearman rank correlation confidence levels of 99.1%). Results for the individual age bins suggest similar inverse correlations, but the correlation is only significant in the intermediate age bin (97.5% confidence). Examining the joint panel illustrates that it is not possible to form large samples of clusters of similar mass with which to examine trends with age. For example, all but seven of the young clusters have masses less than  $5000 M_{\odot}$ , while none of the older clusters have such low masses. Selecting clusters by luminosity mixes lower mass young clusters with higher mass old clusters and so results in a comparison of more massive old systems, with less massive young systems. While our results show that the dependence of ellipticity on mass is more easily identified than any with age, there is a relative deficit of young clusters with very low ellipticity, suggesting that age, and dynamical evolution, may still play a role.

#### 4.1.3. The Irregular Clusters

In Figure 17 we show the images of the 20 clusters with the highest  $\chi_{\nu}^2$  values relative to the King model fitting. These also have high  $\chi_{\nu}^2$  values relative to the EFF model fitting. Several of these clusters are the “ring”-type clusters described above (19, 39, 148, 186), which explains why these are poorly fit by the either profile. Others

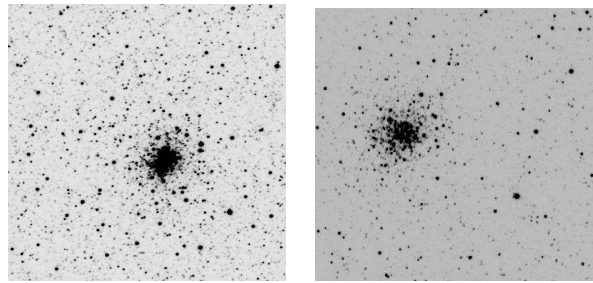


FIG. 15.— V-band images of cluster 98 and 197.

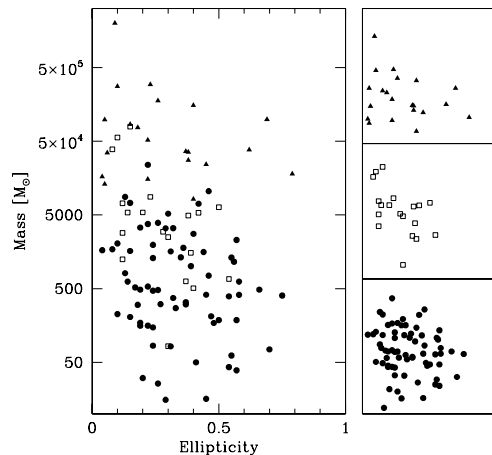


FIG. 16.— Cluster ellipticity vs. mass for three different age bins. The left panel shows all the data, where the youngest clusters are represented with circles, the intermediate age clusters with squares, and the oldest clusters with triangles (see text for defining ages). The right panels separate the three age populations for clarity and rescale to maximize the plot for the relevant population.

have very high central luminosities (70, 71, 181). The remainder appear to suffer from luminosity fluctuations caused by a few stars, which are perhaps unassociated with the cluster. Our principal conclusion is that with the exception of the ring clusters, we find no systematic failure mode for the King and EFF profile fitting. Even in cases where  $\chi_{\nu}^2$  is large, the fits appear to be sufficiently good that one can ascribe the mathematical failure to such systematics as contamination.

#### 4.2. Correlations and Comparisons

We present a set of Spearman rank correlation measures among the cluster parameters we considered (Table 3). Such an exercise can often lead to spurious correlations that are in fact driven by hidden variables, but it can also provide clues to fundamental physical drivers. We discuss a few of the statistically significant correlations that we find interesting. First, we find an inverse correlation between core radius and central surface brightness. Such a correlation would appear to arise naturally among a set of clusters that are dissolving. Second, we find a correlation between the central surface bright-

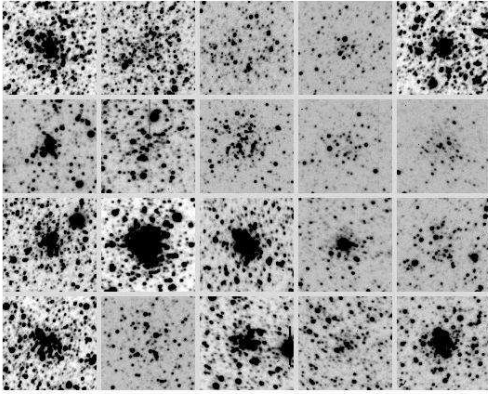


FIG. 17.— V-band images of the twenty clusters with the largest  $\chi^2_\nu$ 's. From upper left across and then down these are clusters 71, 89, 19, 17, 61, 155, 88, 186, 39, 15, 70, 145, 87, 181, 114, 53, 148, 81, 77, and 143.

ness and the background level. This could arise from the practical difficulty in identifying low-surface brightness clusters in denser environments, but could also be due to more efficient disruption of such clusters in higher density regions (Gnedin & Ostriker 1997). These correlations are all internally consistent with a model that has clusters preferentially disrupting in higher density regions. One can only proceed so far on the basis of these correlations. Two key inputs are necessary to continue: 1) ages to disentangle evolutionary effects and 2) models that make quantitative predictions for these correlations. We are currently working on joining the available age estimates (Rafelski & Zaritsky 2004) with model predictions to address these questions.

To complement the internal comparison approach, we also compare the cluster properties to those of Milky Way clusters (data for Galactic clusters from the compilation of Harris (1996)). We present a comparison of the core radii of Milky Way and SMC clusters in Figure 18. The distribution of core radius size is much broader in the SMC than in the MW. This difference is either due to the preferred dissolution of young, low-concentration clusters (both in the SMC and MW) and the preponderance of young clusters in the SMC, or to the preferred formation and survival of lower-concentration clusters in the SMC. The distribution of core radii for clusters with age  $> 1$  Gyr (Figure 18) shows that the older population is just as broad in its distribution of core radii and demonstrates that long-lasting, low-concentration clusters are more prevalent in the SMC than in the MW. Similar results were found for a smaller SMC cluster sample, as well as cluster samples for the LMC, Fornax, and Sagittarius dSphs (Mackey & Gilmore 2004).

## 5. SUMMARY

We present structural parameters for 204 stellar clusters in the Small Magellanic Cloud derived from fitting King and Elson, Fall, and Freeman (EFF) profiles to the V-band surface brightness profiles as measured from the Magellanic Clouds Photometric Survey images. We find that King profiles do a remarkable job at fitting the vast majority of the clusters, which is particularly surprising given that 99% of the clusters will dissolve over

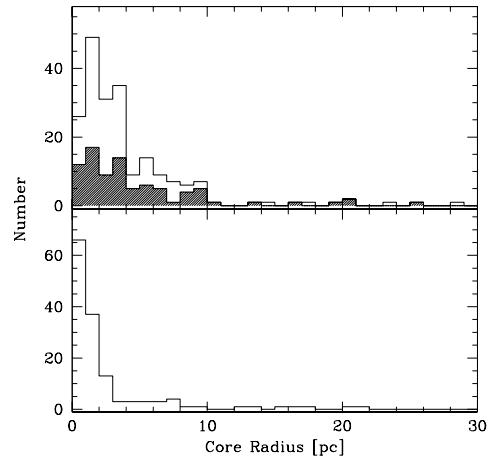


FIG. 18.— The distribution of core radii in the SMC and MW. The SMC distribution is depicted in top panel while that of the MW appears in the bottom panel. In the top panel we also show the distribution for SMC clusters with age  $> 1$  Gyr in the shaded histogram. The MW data come from ?

the next few hundred million years (Rafelski & Zaritsky 2004) and that many have had insufficient time to dynamically relax. We find that the King profiles systematically fit slightly better than the EFF model for most clusters in our sample, independent of cluster age, but that on a cluster by cluster basis it is difficult to rule out one type of model or the other. The only systematic deviation in the surface brightness profiles that we identify is in a set of clusters that lack a central concentration, and which we have named as “ring” clusters. In agreement with previous studies, we find that the clusters in the SMC are significantly more elliptical than those in the Milky Way. We are able to identify an inverse correlation between cluster mass and ellipticity, but find no evidence for one between age and ellipticity. The search for the latter is hampered by the lack of a sizeable sample of clusters with similar masses and a range of ages. We identify several correlations (central surface brightness vs. local background density, size vs. distance) that can be used to constrain models of cluster evolution. Much of the interpretation of the empirical results we present rests on having measured ages and a detailed model for the formation and rapid evolution of the cluster population (extending the models of Bekki et al. (2004)). This current sample of structural parameters provides the basis for detailed studies of the evolution of the cluster system of the Small Magellanic Cloud.

We gratefully acknowledge the referees’ thorough and careful review of this manuscript. AH acknowledges financial support from a NASA Spacegrant. DZ acknowledges financial support from National Science Foundation CAREER grant AST-9733111, AST-0307482, and a fellowship from the David and Lucile Packard Foundation.

TABLE 3  
SPEARMAN RANK CORRELATION PROBABILITIES

Parameter	$r_c$	$r_{90}$	$c_{90}$	Central Den.	Luminosity	Ellipticity	Background
$r_c$	...	.927	-1	-1	1	.741	-.957
$r_{90}$	.927	...	1	-.434	1	-.678	.369
$c_{90}$	-1	1	...	1	-.613	-.659	.951
Central Den.	-1	-.434	1	...	1	-.974	.998
Luminosity	1	1	-.613	1	...	-.991	.909
Ellipticity	.741	-.678	-.659	-.974	-.991	...	-.874
Background	-.957	.369	.951	.998	.909	-.874	...

NOTE. — Probability of correlation between listed cluster properties computed with Spearman rank analysis. Negative sign denotes anti-correlation.

## REFERENCES

- Banks, T., Doff, R. J., & Sullivan, D. J. 1995, MNRAS, 272, 821  
 Bekki, K., Beasley, M. A., Forbes, D.A., & Couch, W. J. 2004, ApJ, 602, 730  
 Bertin, E., & Arnouts, S. 1996, A&AS, 117, 393  
 Bica, E., & Dutra, C.M. 2000, AJ, 119, 1214  
 Bica, E.L.D., Schmitt, H.R., Dutra, C.M., and Oliveira, H.L. 1999, AJ, 117, 238  
 Binney, J., & Tremaine, S. 1987, *Galactic Dynamics*, (Princeton Univ. Press; Princeton)  
 Boutloukos, S.G., & Lamers, H.J.G.L.M. 2003, MNRAS, 338, 717  
 Da Costa, G. S., & Freeman, K. C. 1976, ApJ, 206, 128  
 Elson, R.A.W. 1991, ApJS, 76, 185  
 Elson, R.A.W., Fall, S.M., & Freeman, K.C. 1987, ApJ, 323, 54  
 Elson, R.A.W., Freeman, K.C., & Lauer, T.R. 1989, ApJ, 347, L69  
 Frenk, C.S., & Fall, S.M. 1982, MNRAS, 199, 565  
 Goodwin, S. P. 1997, MNRAS, 286, L39  
 Gnedin, O. Y., & Ostriker, J. P. 1997, ApJ, 474, 223  
 Grillmair, C. J., Freeman, K.C., Irwin, M. & Quinn, P.J. 1995, AJ, 109, 2553  
 Gunn, J.E., & Griffin, R.F. 1979, AJ, 84, 752  
 Han, C., & Ryden, B. S. 1994, ApJ, 433, 80  
 Harris, W. E. 1996, AJ, 112, 1487  
 Harris, J. & Zaritsky, D. 1999, AJ, 117, 2831  
 Holland, S., Coté, P., & Hesser, J. E. 1999, *aj*, 348, 418  
 Holtzman, J.A. et al. 1992, AJ, 103, 691  
 King, I. 1962, AJ, 67, 471  
 King, I. 1966, AJ, 71, 64  
 Kontizas, M., Danezis, E., & Kontizas, E. 1982, A&AS, 49, 1  
 Kontizas, E. & Kontizas, M. 1983, A&AS, 52, 143  
 Kontizas, M., Theodossiou, E., & Kontizas, E. 1986, A&AS, 65, 207  
 Leitherer et al. 1999, ApJS, 123, 3  
 Lupton, R.H., Fall, S.M., Freeman, K.C., and Elson, R.A.W. 1989, ApJ, 347, 201L  
 Lupton, R. H., & Gunn, J. E. 1987, AJ, 93, 11106  
 Lupton, R. H., Gunn, J. E., & Griffin, R. F. 1987, AJ, 93, 1114  
 Mackey, A.D., & Gilmore, G.F. 2003a, MNRAS, 338, 85  
 Mackey, A.D., & Gilmore, G.F. 2003b, MNRAS, 338, 120  
 Mackey, A.D., & Gilmore, G.F. 2004, MNRAS, 355, 504  
 Michie, R. W. 1963, MNRAS, 125, 127  
 Pietrzyński, G., Udalski, A., Kubiak, M., Szymański, M., Woźniak, P. & Zebruń, K. 1998, Acta Astron., 48, 175  
 Prendergast, K.H., & Tomer, E. 1970, AJ, 80,427  
 Rafelski, M., & Zaritsky, D. 2004, AJ, submitted  
 van den Bergh, S. 1981, A&AS, 46, 79  
 van den Bergh, S., & Morbey, C.L. 1984, ApJ, 283, 598  
 Webbink, R. F. 1985, in IAU Symp. 113 Dynamics of Star Clusters, ed. J. Goodman & P. Hut (Dordrecht:Reidel), 541  
 Whitmore, B.C., Schweizer, F., Leitherer, C., Borne, K., & Robert, C. 1993, AJ, 106, 1354  
 Whitmore, B.C., Zhang, Q., Leitherer, C., Fall S.M., Schweizer, F., Miller, B.W. 1999, AJ, 118, 1551  
 Wilson, C. P. 1975, AJ80, 175  
 Wiyanto, P., Kato, S., & Inagaki, S. 1985, PASJ, 37, 715  
 Yang, Y., Zabludoff, A. I., Zaritsky, D., Lauer, T. R., & Mihos, J. C. 2004, ApJ, 608, 358  
 Zaritsky, D., Harris, J., & Thompson, I. 1997, AJ, 114, 1002  
 Zaritsky, D., Harris, J., Thompson, I., Grebel, E.K., & Massey, P. 2002, ApJS,  
 Zaritsky, D., Sheckman, S.A., & Bredthauer, G 1996, PASP, 108, 104